IOP Publishing Phys. Med. Biol. 65 (2020) 075003 (15pp) https://doi.org/10.1088/1361-6560/ab7107

Physics in Medicine & Biology

IPEM Institute of Physics and Engineering in Medicine

OPEN ACCESS

PAPER

Calculated beam quality correction factors for ionization chambers in MV photon beams

J Tikkanen[1,2], K Zink[3], M Pimpinella[4], P Teles[5], J Borbinha[5], J Ojala[6,7], T Siiskonen[1,2], C Gomà[8] and M Pinto[4]

[1] Radiation and Nuclear Safety Authority (STUK), Helsinki, Finland
[2] Helsinki Institute of Physics, University of Helsinki, Helsinki, Finland
[3] Technische Hochschule Mittelhessen—University of Applied Sciences (THM), Gießen, Germany
[4] Italian National Institute of Ionizing Radiation Metrology (ENEA), Research Center Casaccia, Rome, Italy
[5] Grupo de Proteção e Segurança Radiológica, Centro de Ciências e Tecnologias Nucleares, Instituto Superior Técnico (IST), Bobadela, Portugal
[6] Medical Imaging Center, Department of Medical Physics, Tampere University Hospital, Tampere, Finland
[7] Department of Oncology, Tampere University Hospital, Unit of Radiotherapy, Tampere, Finland
[8] Department of Radiation Oncology, Hospital Clínic de Barcelona, Barcelona, Spain

E-mail: joonas.tikkanen@stuk.fi

RECEIVED 31 October 2019

REVISED 24 January 2020

ACCEPTED FOR PUBLICATION 28 January 2020

PUBLISHED 26 March 2020

Keywords: beam quality correction factor, k_Q, volume averaging, Monte Carlo, ICRU-90

Supplementary material for this article is available online

Abstract

The beam quality correction factor, k_Q, which corrects for the difference in the ionization chamber response between the reference and clinical beam quality, is an integral part of radiation therapy dosimetry. The uncertainty of k_Q is one of the most significant sources of uncertainty in the dose determination. To improve the accuracy of available k_Q data, four partners calculated k_Q factors for 10 ionization chamber models in linear accelerator beams with accelerator voltages ranging from 6 MV to 25 MV, including flattening-filter-free (FFF) beams. The software used in the calculations were EGSnrc and PENELOPE, and the ICRU report 90 cross section data for water and graphite were included in the simulations. Volume averaging correction factors were calculated to correct for the dose averaging in the chamber cavities. A comparison calculation between partners showed a good agreement, as did comparison with literature. The k_Q values from TRS-398 were higher than our values for each chamber where data was available. The k_Q values for the FFF beams did not follow the same $TPR_{20,10}$, k_Q relation as beams with flattening filter (values for 10 MV FFF beams were below fits made to other data on average by 0.3%), although our FFF sources were only for Varian linacs.

1. Introduction

Worldwide reference dosimetry in high-energy radiation therapy photon beams is mostly performed by means of ionization chambers calibrated in terms of absorbed dose-to-water (D_w) in a Co-60 beam and applying beam quality correction factors, k_Q, to account for the variation of the ionization chamber response between the calibration and the clinical beam. According to cavity theory, k_Q factors have been expressed in the IAEA TRS-398 protocol (2000) (Andreo *et al* 2001) in terms of Spencer–Attix water-to-air stopping power ratios and several perturbation factors that were originally defined in the previous air-kerma dosimetry protocols (for example IAEA TRS-277 (1987)). Accordingly, the sets of k_Q values included into the TRS-398 protocol, as well as in the AAPM TG-51 (Almond *et al* 1999) protocol, were obtained using theoretical and experimental basic data that were available at the time of the protocol development in the late nineties.

Since the first publication of the above-mentioned D_w dosimetry protocols, problems have been raised both on the formalism and the basic data adopted for the k_Q calculations. Firstly, Sempau *et al* (2004) clarified that the validity of the k_Q expression based on cavity theory implies a number of approximations, such as the independence of the various individual perturbation factors and the absence of correlation between stopping power ratios and perturbation effects. To overcome such approximations, Sempau *et al* (2004) suggested an alternative

approach for determining k_Q, based on Monte Carlo calculation of a single correction factor converting the mean absorbed-dose-to-air in the chamber cavity into absorbed dose-to-water at the reference measurement point. According to this alternative approach, the k_Q factor for beam quality Q can be directly obtained as ratio

$$k_Q = \frac{(D_w/D_{chamber})_Q}{(D_w/D_{chamber})_{Q_0}} \quad (1)$$

where $D_{chamber}$ is the absorbed dose-to-air in the chamber cavity, D_w is the dose-to-water at the reference point, and Q_0 refers to the reference radiation quality. (The symbol k_Q is used instead of k_{Q,Q_0} since the reference beam quality in this work is a Co-60 beam.) Secondly, improvements in computing power and availability of advanced Monte Carlo codes allowed to point out inaccuracies in determining some individual perturbation factors such as p_{wall} and p_{dis} (p_{repl} in the AAPM TG-51) that account for the non-water equivalence of the ionization chamber wall, and for the effects due to the replacement of water with the air cavity, respectively (Buckley and Rogers 2006, Wang and Rogers 2008, Wulff *et al* 2008a, Wang and Rogers 2009). Specifically for photon beams, Monte Carlo simulations by Buckley and Rogers (2006) demonstrated that the semi-empirical expression adopted to calculate p_{wall} does not accurately describe the chamber wall effects. Furthermore, Monte Carlo calculations by Wang and Rogers (2009) revealed that there was an incorrect normalization in the old experimental data on which the TRS-398 p_{dis} values were based. New refined experimental determinations provided p_{dis} values in agreement with the calculated values both in Co-60 and in high-energy photon beams (Swanpalmer and Johansson 2011, 2012), then confirming the reliability of the related Monte Carlo simulations. All these findings have posed the need for a re-evaluation of the recommended values of k_Q.

Muir and Rogers (2010) used the EGSnrc Monte Carlo system to directly calculate k_Q factors for a large number of ionization chambers in photon beams. Their results showed that the Monte Carlo k_Q values differed from the corresponding TRS-398 values up to about 1%. Depending on the chamber type and beam quality, these differences could be explained in terms of variations in the many parameters entering the traditional k_Q expression when calculated using Monte Carlo simulations. A later analysis (Andreo *et al* 2013) of data available for a graphite walled ionization chamber widely used for reference dosimetry in radiation therapy, the NE 2571 type, showed that the Monte Carlo k_Q values were systematically lower than the TRS-398 values with differences increasing up to about 0.8% at the highest photon beam energies. On the other hand, a comparison of the Monte Carlo calculated values with the experimental k_Q data curve, obtained fitting results of measurements performed with different types of D_w primary standards, also showed systematic differences, which indicates the need for further investigation.

In this context, in 2016 the IAEA started a process for the updating of the TRS-398 protocol, including the tables of k_Q values therein. Importantly, the update of the TRS-398 should take into account new modalities of radiation therapy treatment, new ionization chambers on the market, and possible improvements in dosimetric accuracy. In order to establish new recommended values of k_Q, laboratories around the world were invited to submit to the IAEA measured or Monte Carlo calculated k_Q factors with their estimated uncertainties. Then, nine European laboratories interested in contributing to the TRS-398 update set up a consortium with the aim to improve robustness of their k_Q determinations through cooperation in the framework of a metrology project named RTNORM. In this paper, Monte Carlo simulations for megavoltage photon beams made by four laboratories participating in the RTNORM project are described and results are discussed in comparison with literature data.

For k_Q calculations, a number of reference-class cylindrical ionization chambers from different manufacturers, and with different sensitive volumes were considered (table 1). For sources, 20 photon beams from 6 MV to 25 MV, including flattening filter free (FFF) beams, produced by various types of clinical linear accelerators (linacs) as well as two Co-60 beams were used. Settings of radiation transport parameters were initially agreed and chosen so to perform the most accurate simulations. The recent recommendations of the ICRU report 90 (ICRU-90) on key data for reference dosimetry were adopted. Calculations were mostly performed with the EGSnrc code (Kawrakow *et al* 2017) but for two types of ionization chambers the PENELOPE code (Salvat 2015) was used and results compared to each other. The cooperation among the participating laboratories allowed an extensive investigation on approximations and parameters possibly affecting the Monte Carlo calculations. Specifically, the impact on k_Q results of chamber modeling, type of input beam source and approximations in calculating point absorbed dose-to-water were investigated, and critical aspects in the Monte Carlo simulations have been identified and discussed.

2. Methods

ENEA, THM and STUK calculated the k_Q values with EGSnrc user code egs_chamber (Wulff *et al* 2008b), while IST performed their calculations with PENELOPE user code penEasy (Sempau *et al* 2011, Salvat 2015). The

Table 1. Ionization chambers under investigation.

Chamber	Nominal volume (cm^3)	Central electrode	Wall material	Calculated by
Exradin A12S	0.24	C552	C552	IST
Exradin A1SL	0.053	C552	C552	THM
IBA CC13	0.13	C552	C552	ENEA
IBA FC65-G	0.65	Al	Graphite	ENEA, STUK
IBA FC65-P	0.65	Al	POM	ENEA
NE 2571	0.6	Al	Graphite	THM, ENEA, STUK, IST
PTW 30013	0.6	Al	PMMA, graphite	THM, ENEA
PTW 31010	0.125	Al	PMMA, graphite	THM
PTW 31013	0.3	Al	PMMA, graphite	THM
PTW 31021	0.07	Al	PMMA, graphite	THM, STUK

chambers were modeled according to product catalogs and blueprints provided by the manufacturers. Every partner modeled their chambers independently.

The chamber calculations were performed in a 30 cm × 30 cm × 30 cm water-phantom without walls. The source to surface distance (SSD) was 100 cm for linacs. The depth of the reference point of the chamber was at 5 g cm^{-2} for Co-60 sources, and 10 g cm^{-2} for linacs for THM, and at 5 cm and 10 cm for ENEA, STUK and IST. The depth differed, since the density of water in ICRU-90 was 0.9982 g cm^{-3}. The field size at 100 cm was 10 cm × 10 cm for each linac. The dose-to-water was scored to a 0.025 cm thick disk with 1 cm radius by IST and THM. For Farmer-type chambers, ENEA used the same disk dimensions, or a smaller disk radius of 0.25 cm for the CC13 chamber type. For STUK, the dose-to-water was scored in FC65-G and PTW 31021 chamber cavity shaped water volumes.

The chambers under investigation are listed in table 1. All chambers were waterproof, except the NE 2571, which had a 1 mm layer of PMMA on top. The PTW chamber walls consisted of an inner graphite layer surrounded by a thicker layer of PMMA. The charge collection efficiency was assumed to be homogeneous throughout the cavity volumes.

While the amorphous density of graphite used in the calculations was 1.7 g cm^{-3}, the evaluation of the density effect used the crystalline density of 2.265 g cm^{-3}. While ICRU-90 does not make an explicit recommendation, in this work the multiconfiguration Dirac–Fock re-normalization factors for photoelectric cross sections (mcdf-xcom) were used.

2.1. Radiation sources

Point sources with linac energy spectrum, fully simulated linacs and Co-60 irradiators were used in the calculations. Part of the sources are presented in Mohan *et al* (1985), Picard *et al* (2010, 2011, 2013) and Czarnecki *et al* (2017). In addition, a Co-60 source and a Varian TrueBeam linac (Varian Medical Systems, Inc., Palo Alto, California, USA) were modeled with the EGSnrc user code BEAMnrc. Either phase-space files (PSF) or BEAMnrc shared library simulation sources (Kawrakow and Walters 2006), later referred to as BEAM sources, were used in egs_chamber as full linac sources. A list of the sources is in table 2.

ENEA, IST and THM used a BEAMnrc input file for Eldorado Co-60 irradiator available in the IAEA phase-space database Muir *et al* (2009), based on the work in Mora *et al* (1999), as the reference source. The input file was used to create a PSF at 80.5 cm distance from the source. STUK used a BEAMnrc model of their Gammabeam X200 Co-60 irradiator (GBX200) manufactured by Best Theratronics Ltd. (Ottawa, Canada) as the reference source. The source radius was 1 cm and it was encapsulated in a stainless steel container. The collimation consists of a stationary tungsten primary definer, and adjustable lead collimator leaves and tungsten trimmer bars. The scoring plane was at 95 cm from the source and the field size was 10 cm × 10 cm at 100 cm. No variance reduction techniques (VRTs) were used in the GBX200 simulations. A more detailed description and validation of the GBX200 BEAMnrc model will be discussed in a separate study. The SSD corresponded to the BEAMnrc scoring plane distance for both Co-60 sources.

BEAMnrc simulation sources for Varian TrueBeam linac photon beams were based on PSF provided by the manufacturer. The simulated radiation qualities were 6X, 6X-FFF, 10X, 10X-FFF and 15X. The PSFs were collected at a plane above the jaws, and were used as a source in subsequent BEAMnrc treatment head simulation. The input file contained the jaws, an approximation of the collimator baseplate, the MLC in park position, the light field reticle, and the interface mount with the geometrical and material details provided by the manufacturer. The scoring plane was 100 cm from the source for each beam. In all TrueBeam simulations EGSnrc code package version 2018 was used, with simulation parameters shown in table 3 with the exceptions ECUT = AE = 0.521 MeV, PCUT = AP = 0.01 MeV and Brems cross sections = NRC.

Table 2. Sources used in the calculations. The source type for each partner is given in the parenthesis.

Source	$TPR_{20,10}$	Calculated by
Eldorado Co-60 (IAEA database)		ENEA (PSF), IST (PSF), THM (PSF)
Gammabeam X200 Co-60		STUK (BEAM)
Varian TrueBeam 6X-FFF	0.6211	IST (PSF), STUK (BEAM), THM (PSF)
Varian iX 6 MV (IAEA database)	0.6629	ENEA (PSF)
Varian TrueBeam 6X	0.6643	IST (PSF), STUK (BEAM), THM (PSF)
Saturne 43 6 MV (Picard *et al* 2013)	0.6681	ENEA (PSF)
Mohan 6 MV (Mohan *et al* 1985)	0.6702	THM (point source)
Elekta Precise 6 MV, NRC (Picard *et al* 2010)	0.6711	ENEA (PSF), IST (PSF), THM (PSF)
Elekta Precise 6 MV, PTB (Picard *et al* 2011)	0.6839	STUK (PSF), THM (BEAM)
Varian Clinac 10X-FFF (Czarnecki *et al* 2017)	0.6892	THM (BEAM)
Varian TrueBeam 10X-FFF	0.6955	IST (PSF), STUK (BEAM), THM (PSF)
Elekta Precise 10 MV, PTB (Picard *et al* 2011)	0.7303	THM (PSF)
Elekta Precise 10 MV, NRC (Picard *et al* 2010)	0.7306	ENEA (PSF)
Mohan 10 MV (Mohan *et al* 1985)	0.7306	THM (point source)
Varian TrueBeam 10X	0.7341	IST (PSF), STUK (BEAM), THM (PSF)
Saturne 43 12 MV (Picard *et al* 2013)	0.7463	ENEA (PSF)
Varian TrueBeam 15X	0.7558	IST (PSF), STUK (BEAM), THM (PSF)
Mohan 15 MV (Mohan *et al* 1985)	0.7634	THM (point source)
Saturne 43 20 MV (Picard *et al* 2013)	0.7786	ENEA (PSF)
Elekta Precise 25 MV, PTB (Picard *et al* 2011)	0.7979	THM (BEAM)
Elekta Precise 25 MV, NRC (Picard *et al* 2010)	0.7989	ENEA (PSF)
Mohan 24 MV (Mohan *et al* 1985)	0.8045	THM (point source)

The BEAMnrc linac head model for the Elekta Precise accelerator (Elekta Instrument AB, Stockholm, Sweden) was provided by PTB Germany. It was modeled according to the blueprints provided by Elekta. The linac head model and resulting phase space files were evaluated in a BIPM key comparison (Picard *et al* 2011). A Varian Clinac 10X-FFF BEAMnrc simulation source, described in Czarnecki *et al* (2017), was also used in the calculations.

2.2. Beam quality specifier

The beam quality specifier chosen for this work was the $TPR_{20,10}$, which was calculated with equation from Followill *et al* (1998)

$$TPR_{20,10} = 1.2661 PDD_{20,10} - 0.0595, \quad (2)$$

where $PDD_{20,10}$ is the ratio of dose-to-water at depths 20 cm and 10 cm with 100 cm SSD at 10 cm × 10 cm field size. The reason for using the conversion from $PDD_{20,10}$ to $TPR_{20,10}$ was that most of the PSF were scored at a distance larger than 80 cm from the source, and hence the $TPR_{20,10}$ could not be calculated by definition. Since (2) was derived from with-flattening-filter beam data, $TPR_{20,10}$ for the TrueBeam FFF sources was calculated also by definition. The scoring volume for $TPR_{20,10}$ calculations was a 0.25 cm thick disk with radius of 0.5 cm for ENEA and STUK and the 0.025 cm high disk with 1 cm radius for others.

2.3. Simulation parameters and variation reduction techniques in EGS

In the k_Q simulations in EGSnrc, the photons were simulated until the energy was below 1 keV (PCUT and AP) and electrons until 512 keV (ECUT and AE), corresponding to 1 keV kinetic energy. A list of the Monte Carlo parameters, unless mentioned otherwise, is in table 3.

The egs_chamber user code provides multiple effective VRTs that speed up the calculations significantly, and enable extracting more information from a limited number of particles. These techniques are presented in Wulff *et al* (2008b). One such technique is the photon cross-section enhancement (XCSE), where the photon total cross section is increased by an enhancement factor n in a volume surrounding the chamber cavity. The secondary particle weights are reduced by the same factor and photon interactions are carried out with probability $1/n$. This leads to a situation where higher number of electrons, with reduced weight, are created along the track of a photon.

In Russian Roulette (RR), when an electron is created, the program checks whether a user defined geometry is within the electron range. If not, the electron is simulated only with probability $1/m$, where m is a rejection factor, and the weight is multiplied by m. Simulating part of the electrons will take into account the contribution to dose from x-rays generated by the electrons. If the electron is inside the volume, it is terminated and energy deposited

Table 3. Monte Carlo transport parameters for the EGSnrc simulations.

Global ECUT	0.512
Global PCUT	0.001
Global SMAX	1e10
ESTEPE	0.25
XImax	0.5
Skin depth for BCA	3
Boundary crossing algorithm	EXACT
Electron-step algorithm	PRESTA-II
Spin effects	On
Brems angular sampling	KM
Brems cross sections	NIST
Photon cross sections	mcdf-xcom
Electron impact ionization	On
Triplet production	On
Radiative Compton corrections	On
Bound Compton scattering	On
Pair angular sampling	KM
Pair cross sections	NRC
Photoelectron angular sampling	On
Rayleigh scattering	On
Atomic relaxations	On
Photonuclear attenuation	On

in the current region if the electron energy is below an Esave parameter. The material with which the electron ranges are calculated is given as a input and it should be the least attenuating material around the chamber cavity. If there is air outside the chamber cavity, it is more effective to expand the RR region around those areas than define the rejection material as air.

In intermediate phase-space scoring (IPSS), an intermediate phase-space is scored on a surface of a defined geometry. These scored particles are then transported to every other geometry in the scoring options block in the input file. This can be convenient when simulating multiple geometries at the same position.

ENEA used an XCSE region surrounding the chamber geometries by 2 cm, and an enhancement factor of 128 for Co-60 and 6 MV beams and 64 for other beams. The RR rejection factor was equal to the enhancement factor and the Esave parameter was 521 keV. STUK had a XCSE enhancement factor of 64 and rejection factor of 128 for all calculations. The Esave parameter was 512 keV. THM applied for all simulations a XCSE factor of 128 (equal to the RR rejection factor) within a region of 2 cm surrounding the individual chamber geometries and the ESAVE parameter was 521 keV. To save computation time, STUK and THM applied the IPSS technique and simulated all the chambers in one run. The IPSS volume encompassed all XCSE volumes.

2.4. Simulation parameters and variation reduction techniques in PENELOPE

The penEasy version in the calculations was 2015-05-13 (compatible with the PENELOPE 2014 code package). The use of PENELOPE and penEasy for calculating k_Q and $TPR_{20,10}$ factors has been studied for example in Sempau and Andreo (2006), Erazo and Lallena (2016), Gomà *et al* (2016). Material files in accordance with ICRU-90 were used and the mean excitation energies were set to 81 eV and 78 eV for graphite and water, respectively.

The detailed geometries of the ionization chambers were designed by means of quadratic surfaces using the PENELOPE package PENGEOM (Salvat 2015). The chambers implemented in PENELOPE were NE 2571 and Exradin A12S. Both chamber geometries were modeled according to manufacturer's specifications and literature (Erazo and Lallena 2013, Pimpinella *et al* 2019). The tallyEnergyDeposition was used to calculate the energy deposited in the chamber cavity and in water.

PENELOPE uses various parameters for electron and positron transport: C1 (average angular deflection produced by multiple scattering), C2 (maximum average fractional energy loss between consecutive hard inelastic events), Wcc (cutoff energy for hard inelastic collisions) and Wcr (cutoff energy for hard bremsstrahlung emission). DSMAX refers to the maximum step length of charged particles in the materials. Typically, this parameter is set to approximately 0.1 times the material thickness (Salvat 2015). For both chambers, detailed simulation (C1 = C2 = Wcc = Wcr = 0) was performed in the active volume, as well as in all regions sharing a surface with it. For other materials in the chamber and water present up to 2 cm around the chamber, the parameters C1 and C2 were set to 0.05. In the water phantom and surrounding air, C1 and C2 were 0.1. Wcc and Wcr had values of 10 keV and 1 keV, respectively, for all materials, except the ones where detailed simulation was performed. Additionally,

Table 4. Comparison of the k_Q factors calculated for NE 2571 in a 6 MV Elekta Precise beam provided by NRC (Picard *et al* 2010). The type A standard uncertainties are given in columns $\delta\text{TPR}_{20,10}$ and δk_Q, and $\Delta\text{TPR}_{20,10}$ and Δk_Q are the differences to the median.

Partner	$\text{TPR}_{20,10}$	$\delta\text{TPR}_{20,10}$ (%)	$\Delta\text{TPR}_{20,10}$ (%)	k_Q	δk_Q (%)	Δk_Q (%)
ENEA	0.6715	0.07	0.031	0.9916	0.09	0.019
IST	0.6684	0.21	−0.44	0.9944	0.18	0.3
STUK	0.6712	0.11	−0.019	0.9912	0.13	−0.019
THM	0.6715	0.04	0.019	0.9909	0.05	−0.054

DSMAX was set to approximately one tenth of material thickness. For photons, cutoff energy was 1 keV in all materials. For electrons and positrons, cutoff energies were set to 1 keV for all chamber materials, 10 keV for water present up to 2 cm around the chamber and 200 keV for other regions.

The simulations to obtain D_w were performed analogously to the chamber simulations. A 0.5 mm water skin enveloped the dose-to-water scoring volume. Detailed simulation was performed in both of these bodies. The C1, C2, Wcc, Wcr and DSMAX were as in chamber simulations with the region of C1 = C2 = 0.05 enveloping the disk by up to 2 cm.

For all simulations, simple particle splitting was implemented in the sensitive volume, with a factor of 10. Additionally, a SPLITTING FACTOR was used for the phase space sources, equal to 10 for the Varian and NRC's Elekta beams and 200 for the Co-60 beam (the Eldorado Co-60 PSF was much smaller than the other PSF). During the simulation, each particle in the PSF was split and run SPLITTING FACTOR times and the statistical weight was reduced accordingly. However, a very large SPLITTING FACTOR may lead to a stack overflow. To solve this problem, the parameter NMS was modified to 1000 000 in the PENELOPE source files (penEasy v.2015-05-13 documentation, source phase space file. J. Sempau). The splitting factors presented in this section are the result of several trial and error tests performed in an effort to improve simulation efficiency without biasing the simulation results.

2.5. Difference in dose profiles between phase space files and beam sources

When calculating the dose profiles with EGSnrc for the TrueBeam, Eldorado and GBX200 PSFs, the variance between single simulated doses was larger than what would have been predicted by the uncertainties. The effect was observed regardless of whether the PSF were restarted (the PSF run multiple times without reducing the particle weights) or not, making the latent variance of the PSFs an unlikely reason for the behavior (Sempau *et al* 2001, Alhakeem and Zavgorodni 2018). When making identical simulations with BEAM sources, the variance between the points was lower and the results were as expected. THM assumed that the dimensions of the chambers were large enough to average most of the unexpected variance in the profiles and BEAM sources were used whenever possible. Preliminary investigation with PENELOPE did not show unexpectedly large variance in the profile calculations.

2.6. Volume correction factors

Volume correction factors k_{vol}, according to the recommendation of the IAEA report TRS-483 (IAEA 2017) resulting from inhomogeneous dose profiles, were applied to the k_Q by IST and THM. The correction factor converts the average dose throughout the dose calculation volume into the dose at the reference point. The formulae for calculating the k_{vol} factors are presented for example in Delaunay and Ostrowsky (2007) for the simplest methods and analyzed more thoroughly in IAEA TRS-483. The equation for the volume correction factor from the TRS-483 is

$$k_{\text{vol}} = \frac{\iint_A w(x,y)\,\mathrm{d}x\mathrm{d}y}{\iint_A w(x,y)\,\text{OAR}(x,y)\,\mathrm{d}x\mathrm{d}y}, \tag{3}$$

where $w(x,y)$ is the weighting factor that takes into account the calculation volume thickness in the beam direction, and OAR is the off-axis-ratio, meaning the ratio of dose at position (x,y) and at the center of the beam. The simplest method to calculate the correction factor for a cylindrical ionization chamber is a line integral along the chamber axis

$$k_{\text{vol,chamber}} = \frac{L}{\int_{-L/2}^{L/2} \text{OAR}(0,y)\,\mathrm{d}y}, \tag{4}$$

where L is the chamber length and the chamber is aligned along the y-axis. Equation (4) assumes that the dose averaging in radial direction is negligible. For the disk shaped D_w calculation volume, this assumption is not valid

Table 5. Examples of volume correction factors calculated with (4) and (5), and the correction factors applied to the k_Q calculated with average doses over the dose scoring volumes calculated with (7). The partner who applied the correction factor in question is given in brackets.

Beam	Chamber	k_{vol}	k'_{vol}
GBX200	NE 2571	1.0007	
TrueBeam 6X-FFF	D_w (IST)	1.0029	
	Exradin A12S (IST)	1.0005	1.0024
	NE 2571 (IST)	1.0027	1.0003
TrueBeam 10X-FFF	D_w (IST)	1.0057	
	Exradin A12S (IST)	1.0010	1.0047
	NE 2571 (IST)	1.0054	1.0003
Clinac 10X-FFF	D_w (THM)	1.0052	
	Exradin A1SL (THM)	1.0000	1.0052
	NE 2571 (THM)	1.0050	1.0002
	PTW 30013 (THM)	1.0046	1.0006
PTB 10 MV	D_w (THM)	0.9944	
	Exradin A1SL (THM)	0.9981	0.9963
	NE 2571 (THM)	0.9950	0.9994
	PTW 30013 (THM)	0.9951	0.9993
PTB 25 MV	D_w (THM)	0.9948	
	Exradin A1SL (THM)	1.0001	0.9947
	NE 2571 (THM)	0.9951	0.9997
	PTW 30013 (THM)	0.9955	0.9993

Table 6. Fitting parameters of equation (8) for the chambers, calculated using only the WFF beam results. Exradin A12S is not included due to a low number of fitting points.

Chamber	*a*	*b*	*c*
Exradin A1SL	1.012 046	1.177 738	−0.127 2004
IBA FC65-G	1.002 259	1.083 689	−0.089 132 54
IBA FC65-P	1.001 615	1.077 563	−0.089 465 35
IBA CC13	1.009 709	1.164 627	−0.123 3315
NE2571	1.000 877	1.050 988	−0.077 470 78
PTW 30013	1.003 557	1.107 292	−0.102 4183
PTW 31010	1.010 624	1.182 641	−0.133 7003
PTW 31013	1.001 961	1.094 123	−0.095 3281
PTW 31021	1.008 156	1.163 214	−0.119 008

and the volume correction factor was calculated assuming cylindrical symmetry of the profile within the disk radius

$$k_{vol,w} = \frac{\int_0^R \int_0^{2\pi} w(r) r \mathrm{d}r\mathrm{d}\theta}{\int_0^R \int_0^{2\pi} w(r)\mathrm{OAR}(r) r \mathrm{d}r\mathrm{d}\theta} = \frac{R^2}{2\int_0^R \mathrm{OAR}(r) r \mathrm{d}r}, \quad (5)$$

where the weighting factor $w(r) \equiv 1$ since the thickness is constant, R is the disk radius and r the distance from the beam axis.

To obtain the OAR, THM calculated dose-profiles for the sources they used. The volume correction factors were applied to chambers simulated by THM and the profiles were calculated with the egs_chamber user code. The water voxel for the profile calculations was a disk with a radius of 0.1 cm and height of 0.2 cm centered around the measurement depth 10 cm for the high energy photon beams and 5 cm for Co-60. To save calculation time, the calculations were performed applying an ECUT value of 0.521 MeV instead of 0.512 MeV.

Additionally, the profiles of the TrueBeam 6X-FFF and 10X-FFF beams at the 10 cm depth were calculated using a BEAM source and the volume correction factors obtained from these calculations were used by IST. The water voxels for the profile calculations were rectangular parallelepiped with dimensions of 0.1 cm × 0.3 cm × 0.1 cm in *xyz*-directions. The variance reduction parameters were as in section 2.3. Both THM and IST used polynomial fits to the simulated profiles to get the OAR function.

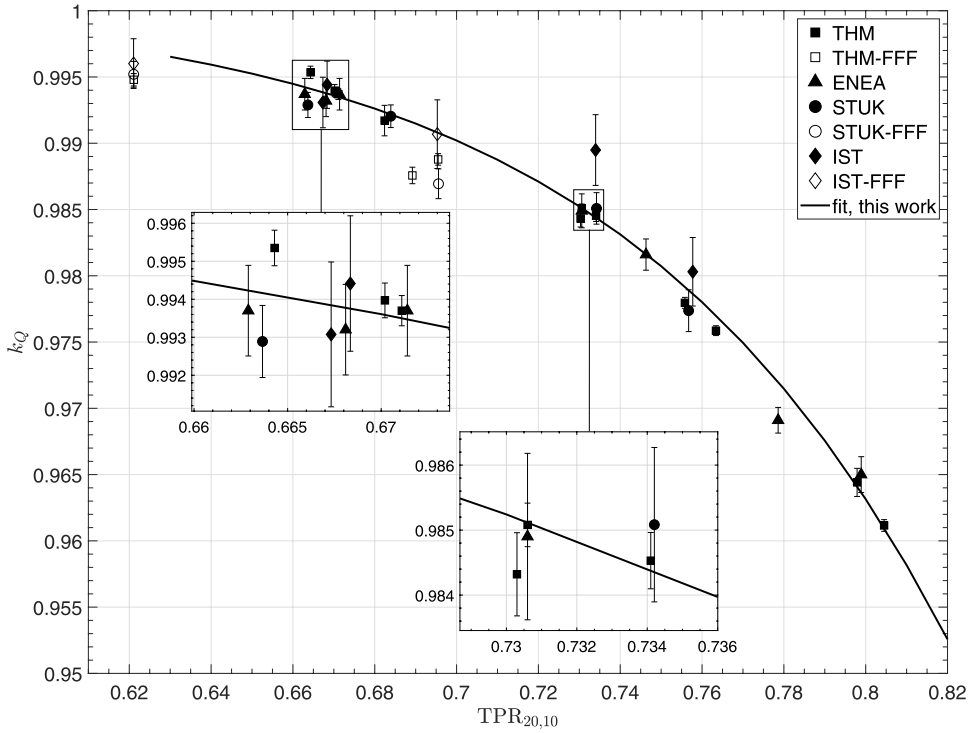

Figure 1. The calculated k_Q factors for the NE 2571 chamber. The error bars represent the type A standard uncertainty. The FFF-beam data was not used in calculation of the fit.

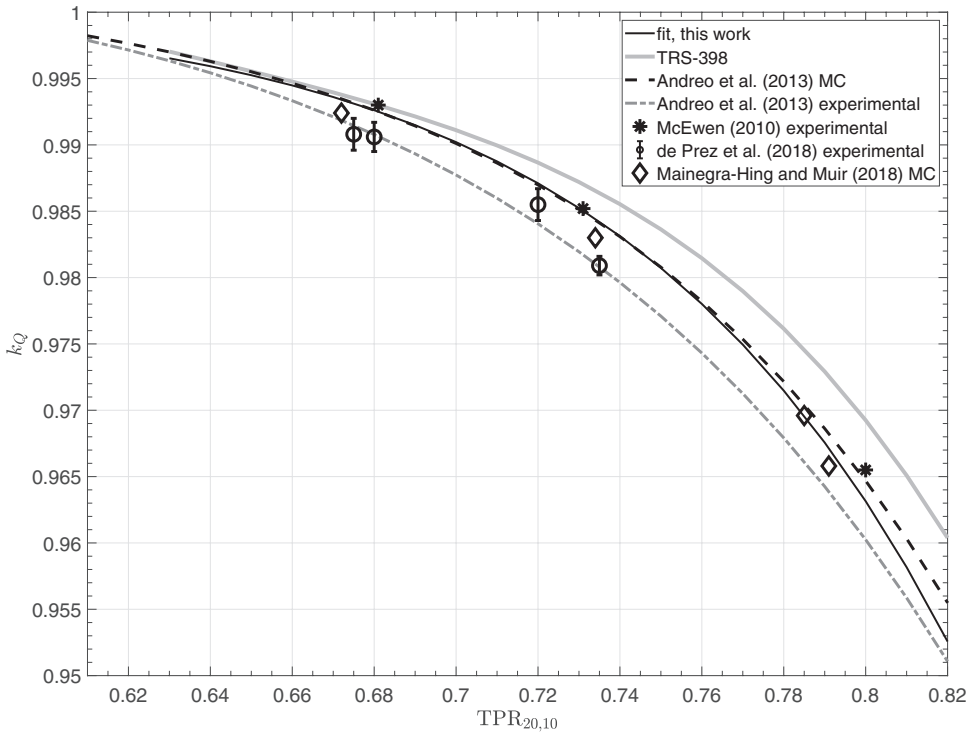

Figure 2. Comparison of the k_Q fit for the NE 2571 chamber to literature.

The measured dose-to-water at reference depth in beam quality Q is given by

$$D_{\mathrm{w,Q}} = M_Q N_{D,\mathrm{w},Q_0} k_Q, \tag{6}$$

where N_{D,w,Q_0} is the calibration coefficient for the dose-to-water measured in a Co-60 beam and M_Q is the dosimeter reading corrected for influence quantities. If these quantities include the volume averaging in the cavity, the D_{chamber} in (1) has to be corrected for the volume averaging. In this case, k_Q corrects only for the difference of the chamber response between the radiation spectra of Q and Q_0. If the volume averaging correction

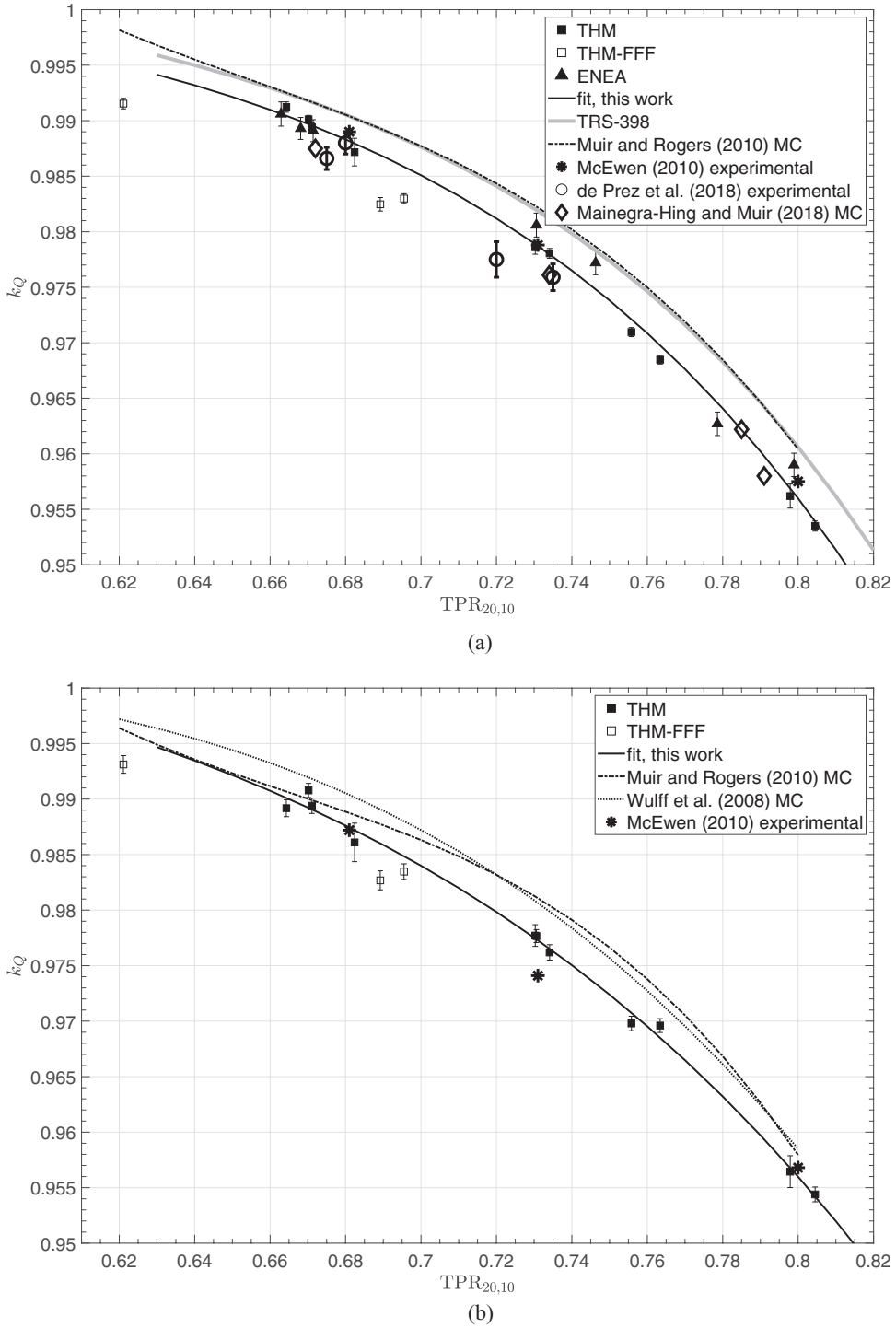

Figure 3. Calculated k_Q factors for the PTW 30013 (a) and PTW 31010 (b) chambers. The error bars represent the type A standard uncertainty. The FFF-beam data was not used in calculation of the fits.

is not included in M_Q, then the average dose over the cavity volume is used in the calculation of k_Q. The dose-to-water is defined at the reference point in both cases, meaning that the volume averaging in the D_w scoring volume is corrected for. The correction factor applied to the k_Q values calculated with simulated (average) doses over both D_w and $D_{chamber}$ scoring volumes can then be obtained with

$$k'_{vol} = \frac{k_{vol,w}}{k_{vol,chamber}}. \quad (7)$$

Note that (7) assumes the volume correction factors for the Co-60 beam to be unity.

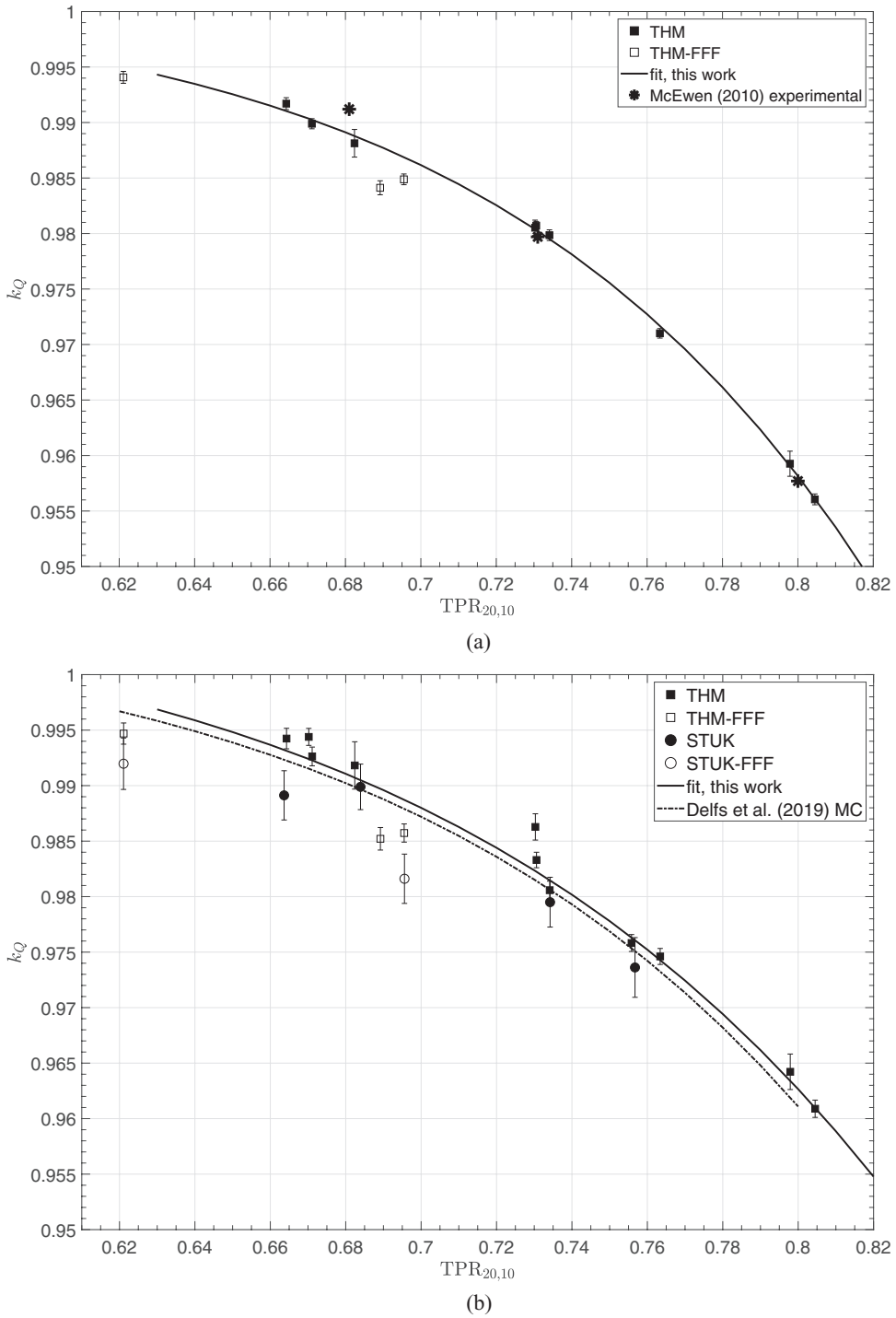

Figure 4. Calculated k_Q factors for the PTW 31013 (a) and PTW 31021 (b) chambers. The error bars represent the type A standard uncertainty. The FFF-beam data was not used in calculation of the fits.

3. Results and discussion

3.1. Comparison of beam quality correction factors for NE 2571 chamber

Each partner calculated the k_Q factor for the NE 2571 chamber with the Eldorado Co-60 PSF and Elekta Precise 6 MV PSF from NRC (Picard *et al* 2010) for validation of the calculation methods. Every partner restarted the PSF (the particles in the file were run multiple times without reducing the weight). The results of the comparison are in table 4. The values of ENEA, STUK and THM, calculated with EGSnrc using matched simulation settings but using independently developed geometries and different realization of the variance reduction techniques, are in agreement within 0.07%. The values of IST calculated using PENELOPE show larger differences compared to the values calculated by the other partners using EGSnrc, although their k_Q value is within the expanded uncertainty from the median result. The type B uncertainties are not included in the uncertainty estimation, and the

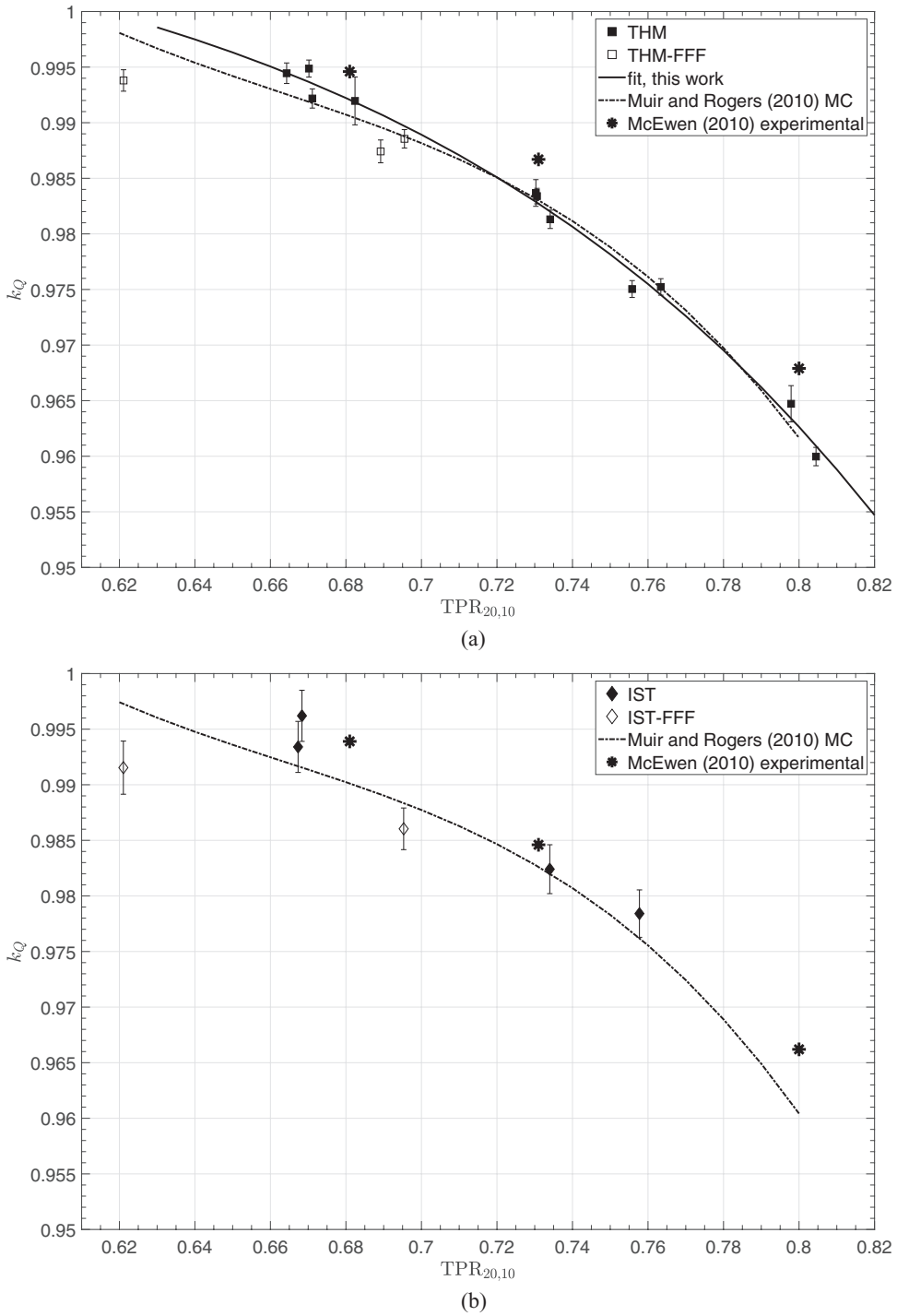

Figure 5. Calculated k_Q factors for the Exradin A1SL (a) and A12S (b) chambers. The error bars represent the type A standard uncertainty. The FFF-beam data was not used in calculation of the fit.

difference between the results might be due to variations in library data. The estimation of type B uncertainties is studied for example in Muir and Rogers (2010), Wulff *et al* (2010), Muir *et al* (2011) and Czarnecki *et al* (2018), and the subject is beyond the scope of this publication. However, based on these studies the type B uncertainty of the Monte Carlo k_Q values can be estimated below 0.5% ($k = 1$). The differences between the comparison results were deemed small enough to regard the calculation methods of each partner valid.

3.2. Volume correction factors

The volume averaging was most significant in the FFF-beams, and in PTB's Elekta Precise 10 MV and 25 MV beams. Because of the more significant dose averaging in the 1 cm radius disk D_w scoring volume than in the cavity, the corrections to the k_Q calculated with averaged doses were largest for the small chambers. Some of the calculated volume correction factors are listed in table 5. STUK did not need to take the volume averaging into

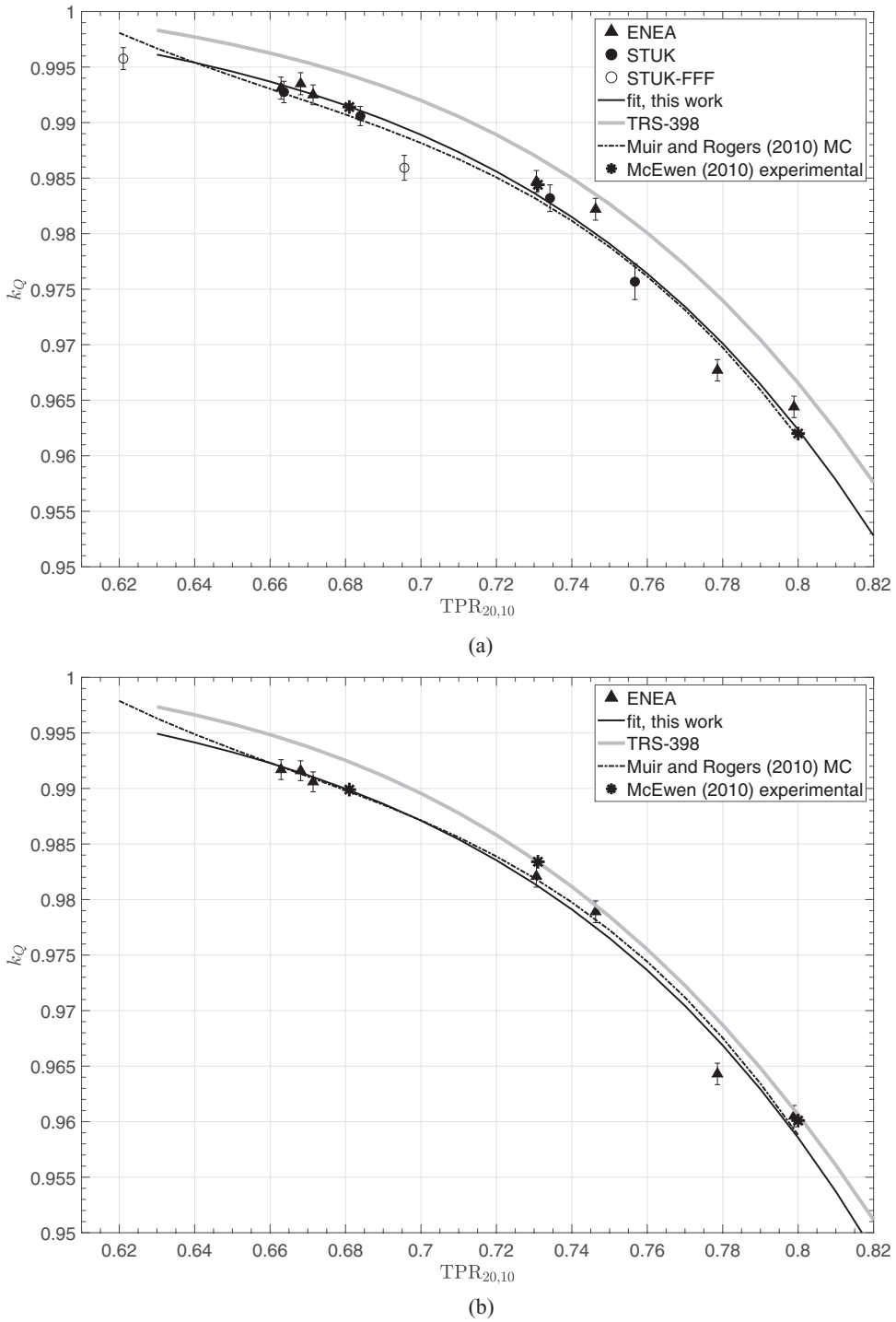

Figure 6. Calculated k_Q factors for the IBA FC65-G (a) and IBA FC65-P (b) chambers. The error bars represent the type A standard uncertainty. The FFF-beam data was not used in calculation of the fit.

account even though FFF beams were used, since the correction factor was the same for the chamber and the cavity shaped dose-to-water scoring volume. The shapes of NE 2571 and FC65-G chamber cavities were close enough to assume the difference between the volume correction factors to be insignificant. ENEA's calculations of k_Q factors showed equal results (within 0.1%) when using dose-to-water scoring volumes matching the chamber cavity or using a disk with diameter matching the chamber cavity length (Pimpinella *et al* 2019). These calculations allowed ENEA to establish that the volume averaging effect can be neglected for the sources and the dose-to-water scoring volumes that they used.

Although (4) uses the simple weighting factor, the k_{vol} factors according to TRS-483 are close to those calculated with more accurate methods. This was verified for the FFF beams by calculating the volume correction factors for NE 2571, FC65-G and A12S chambers with a model that takes into account the chamber cavity shape and the central electrode. The factors agreed to within 0.0003.

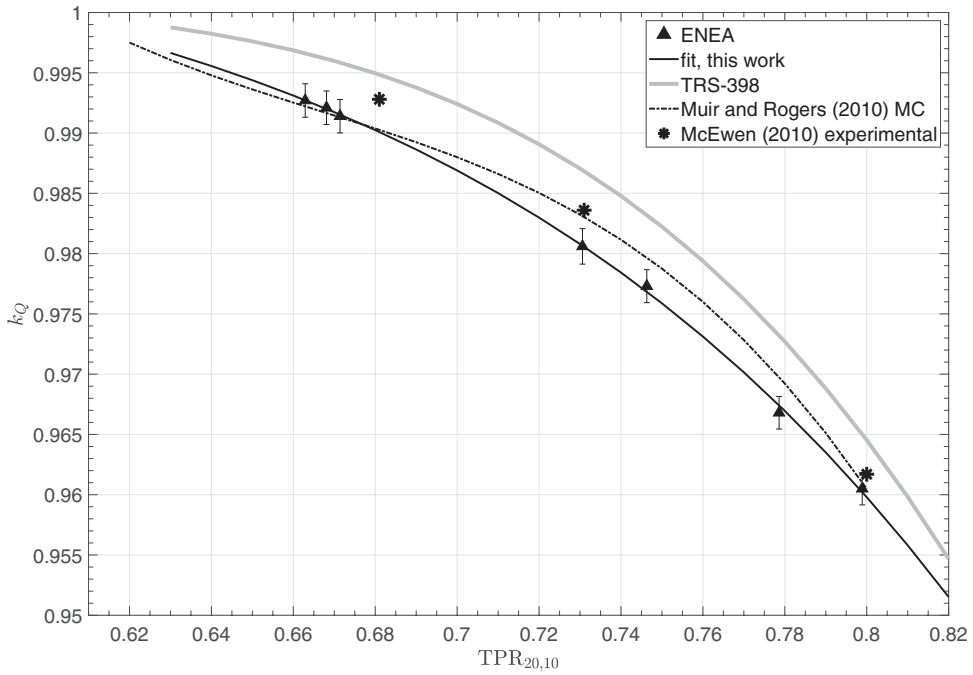

Figure 7. Calculated k_Q factors for the IBA CC13 chamber. The error bars represent the type A standard uncertainty.

3.3. Calculated beam quality correction factors

The calculated beam quality correction factors and comparison to previously published data are shown in figures 1–7. In each figure, the error bars represent the type A standard uncertainty. The uncertainty of the k_Q was calculated by assuming that the uncertainties of individual dose calculations were uncorrelated and the correlated sampling option in egs_chamber was not used. The calculated k_Q factors are given as supplementary material (stacks.iop.org/PMB/65/075003/mmedia).

A fitting function from Andreo *et al* (2013)

$$k_Q = \frac{a}{1 + \exp(\frac{b - \mathrm{TPR}_{20,10}}{c})}, \tag{8}$$

where a, b and c are fitting parameters, was used to obtain fits to the k_Q data. The parameters are given in table 6. The fits do not have any physical meaning and may not be valid outside the $\mathrm{TPR}_{20,10}$ range of the sources used. The FFF-beam data does not follow the same fit as the with flattening filter (WFF) beam data for the 10 MV FFF beams and the FFF points are below the fit. Due to the difference, the FFF-beam results were not used when calculating the fitting parameters. The difference of the FFF-beam k_Q values to the value of the fit at the same $\mathrm{TPR}_{20,10}$ for the 10X-FFF beams averaged per chamber ranged from 0.2% to 0.5% and the average difference over all the chambers was 0.33%. The difference between the WFF and FFF beam k_Q values was not estimated for the 6X-FFF beam since the fit would have had to be extrapolated. If the volume averaging in the chamber cavity had not been corrected for, the FFF and WFF data would be in better agreement. However, we can make no general conclusion of the validity of using the same $\mathrm{TPR}_{20,10}$, k_Q fit for FFF-beams from the results of this work, especially since all the FFF data is for Varian linacs; other manufacturers realise the FFF beams in a different way (de Prez *et al* 2018).

The difference between the $\mathrm{TPR}_{20,10}$ for FFF beams calculated with (2) and by definition was less than 0.004. This difference is well within the expanded uncertainty of approximately 0.009 of the $\mathrm{TPR}_{20,10}$, $\mathrm{PDD}_{20,10}$ relation given in Followill *et al* (1998). When using the fitting parameters for the NE 2571 chamber from table 6, the changes in k_Q between the $\mathrm{TPR}_{20,10}$ calculated by the two different methods were less than 0.05%. Therefore the $\mathrm{TPR}_{20,10}$ values calculated with (2) for the FFF beams used are considered accurate enough for the purposes of this work.

For every chamber, the results between partners are consistent, especially with acceleration voltages of 10 MV and lower, and difference to considered literature, not including TRS-398, is less than approximately 0.5%. For the NE 2571 chamber, the agreement with other calculated k_Q values is good, with difference in figure 2 never exceeding 0.2%. The same level of agreement is found with the experimental determinations from McEwen (2010). Difference to measured values from Andreo *et al* (2013) and de Prez *et al* (2018) is larger, but always below 0.4%. For the PTW 30013 (figure 3(a)), there is a systematic difference between our results and the fit from Muir and Rogers (2010), while there is a good agreement with more recent data from Mainegra-Hing and Muir (2018),

who reportedly modeled in more detail the stem of the chamber, compared to Muir and Rogers (2010). In this study we also paid particular attention to the geometry of this chamber type, and this may possibly explain the better agreement between our results and those of Mainegra-Hing and Muir (2018). This study also shows a systematic difference for PTW 31010 (figure 3(b)) between our results and those of Wulff *et al* (2008a) and Muir and Rogers (2010) at higher $TPR_{20,10}$ values, even though EGSnrc was used in both studies. Of note is that agreement with experimental results from McEwen (2010) is very good for both chambers. The TRS-398 values are higher than ours for each chamber. For the IBA CC13 chamber, the difference is most significant in the TPR range of 6 MV to 10 MV beams. However, our results agree with the data in TRS-398 within the TRS-398 stated standard uncertainty of 1%. The differences are at least partly explained by issues discussed in section 1. For PTW 31021, our results agree well with the results in Delfs *et al* (2019), but the data from STUK is systematically lower than the data from THM. The adaptation of the new ICRU-90 cross sections does not affect the k_Q values significantly based on Czarnecki *et al* (2018) and Mainegra-Hing and Muir (2018).

4. Conclusions

We calculated an extensive dataset of k_Q factors for 10 ionization chambers adding to 147 k_Q values in 20 linac beams. The validity of the results was improved by comparing partner's calculated k_Q and $TPR_{20,10}$ values to each other, and to literature. No systematic differences across chambers to calculated nor measured literature results were observed, with the exception of TRS-398 data, where the k_Q were higher for each chamber where data was available. Part of the chambers have little existing k_Q data and are not included in the current version of TRS-398, for example PTW 31013 and the PTW Semiflex 31021 3D. We used the ICRU-90 cross sections for water and graphite, which only few publications have provided k_Q data with. The FFF-beam results, calculated for two Varian linacs, do not follow the same fit as beams with a flattening filter, at least when the volume averaging in the chamber cavity is corrected in the determination of k_Q. Furthermore, our FFF beams followed the conversion from $PDD_{20,10}$ to $TPR_{20,10}$ from Followill *et al* (1998) within the stated uncertainties of that work.

Acknowledgments

The authors wish to thank NRC, LNHB, PTB and ARPANSA for providing PSF for the Monte Carlo calculations of this work. Special thanks to Ralf-Peter Kapsch from PTB for providing the BEAMnrc head model for the ELEKTA Precise accelerator, and to Antti Kosunen and Franck Delaunay for counsel regarding this work. The authors also thank IBA Dosimetry, PTW and Standard Imaging for providing the blueprints of the chambers.

IST thanks professor Pedro Andreo for providing information about the necessary changes to the code PenEasy for the implementation of the cross-sections for air, graphite, and water in accordance with ICRU 90 data.

This work is part of the RTNORM research project which has received funding from the EMPIR programme, Grant 16NRM03 'k_Q factors in modern external beam radiotherapy applications to update IAEA TRS-398', co-financed by the Participating States and from the European Union's Horizon 2020 research and innovation programme.

Part of the computing resources and the related technical support used for this work have been provided by CRESCO/ENEAGRID High Performance Computing infrastructure and its staff (see www. cresco.enea.it for information).

ORCID iDs

K Zink https://orcid.org/0000-0001-5785-4101
J Ojala https://orcid.org/0000-0002-2476-2419
M Pinto https://orcid.org/0000-0002-8122-7084
C Gomà https://orcid.org/0000-0003-0336-390X

References

Alhakeem E and Zavgorodni S 2018 Evaluation of latent variances in Monte Carlo dose calculations with varian TrueBeam photon phase-spaces used as a particle source *Phys. Med. Biol.* **63** 01NT03

Almond P R, Biggs P J, Coursey B M, Hanson W F, Huq M S, Nath R and Rogers D W O 1999 AAPM's TG-51 protocol for clinical reference dosimetry of high-energy photon and electron beams *Med. Phys.* **26** 1847–70

Andreo P, Burns D T, Hohlfeld K, Huq M S, Kanai T, Laitano F, Smyth V and Vynckier S 2001 *Absorbed Dose Determination in External Beam Radiotherapy. An International Code of Practice for Dosimetry Based on Standards of Absorbed Dose to Water, Technical Reports Series* vol 398 (Vienna: International Atomic Energy Agency)

Andreo P, Wulff J, Burns D T and Palmans H 2013 Consistency in reference radiotherapy dosimetry: resolution of an apparent conundrum when ^{60}Co is the reference quality for charged-particle and photon beams *Phys. Med. Biol.* **58** 6593–621
Buckley L A and Rogers D W O 2006 Wall correction factors, for thimble ionization chambers *Med. Phys.* **33** 455–64
Czarnecki D, Poppe B and Zink K 2017 Monte Carlo-based investigations on the impact of removing the flattening filter on beam quality specifiers for photon beam dosimetry *Med. Phys.* **44** 2569–80
Czarnecki D, Poppe B and Zink K 2018 Impact of new ICRU report 90 recommendations on calculated correction factors for reference dosimetry *Phys. Med. Biol.* **63** 155015
de Prez L, de Pooter J, Jansen B, Perik T and Wittkmper F 2018 Comparison of k_q factors measured with a water calorimeter in flattening filter free (FFF) and conventional flattening filter (cFF) photon beams *Phys. Med. Biol.* **63** 045023
Delaunay F and Ostrowsky A 2007 Some specific features of ionization chamber calibrations in linac x-ray beams at the LNE-LNHB *Phys. Med. Biol.* **52** N207–11
Delfs B, Kapsch R P, Chofor N, Looe H K, Harder D and Poppe B 2019 A new reference-type ionization chamber with direction-independent response for use in small-field photon-beam dosimetry—an experimental and Monte Carlo study *Z. Med. Phys.* **29** 39–48
Erazo F and Lallena A M 2013 Calculation of beam quality correction factors for various thimble ionization chambers using the Monte Carlo code PENELOPE *Phys. Med.* **29** 163–70
Erazo F and Lallena A M 2016 Photon beam quality correction factors for the NE2571A and NE2581A thimble ionization chambers using PENELOPE *Phys. Med.* **32** 232–6
Followill D S, Tailor R C, Tello V M and Hanson W F 1998 An empirical relationship for determining photon beam quality in TG-21 from a ratio of percent depth doses *Med. Phys.* **25** 1202–5
Gomà C, Andreo P and Sempau J 2016 Monte Carlo calculation of beam quality correction factors in proton beams using detailed simulation of ionization chambers *Phys. Med. Biol.* **61** 2389–406
IAEA 1987 Absorbed dose determination in photon and electron beams: an international code of practice *Technical Report* No. 277, (Vienna: International Atomic Energy Agency)
IAEA 2017 Dosimetry of small static fields used in external beam radiotherapy *Technical Reports Series* No. 483 (Vienna: International Atomic Energy Agency) (www.iaea.org/publications/11075/dosimetry-of-small-static-fields-used-in-external-beam-radiotherapy)
Kawrakow I, Mainegra-Hing E, Rogers D W O, Tessier F and Walters B R B 2017 The EGSnrc code system: Monte Carlo simulation of electron and photon transport *Technical Report* PIRS-701 (Ottawa: National Research Council Canada) (http://nrc-cnrc.github.io/EGSnrc/doc/pirs701-egsnrc.pdf)
Kawrakow I and Walters B R B 2006 Efficient photon beam dose calculations using DOSXYZnrc with BEAMnrc *Med. Phys.* **33** 3046–56
Mainegra-Hing E and Muir B R 2018 On the impact of ICRU report 90 recommendations on *kq* factors for high-energy photon beams *Med. Phys.* **45** 3904–8
McEwen M R 2010 Measurement of ionization chamber absorbed dose factors in megavoltage photon beams *Med. Phys.* **37** 2179–93
Mohan R, Chui C and Lidofsky L 1985 Energy and angular distributions of photons from medical linear accelerators *Med. Phys.* **12** 592–7
Mora G M, Maio A and Rogers D W O 1999 Monte Carlo simulation of a typical therapy source *Med. Phys.* **26** 2494–502
Muir B R and Rogers D W O 2010 Monte Carlo calculations of *kq*, the beam quality conversion factor *Med. Phys.* **37** 5939–50
Muir B R, McEwen M R and Rogers D W O 2011 Measured and Monte Carlo calculated *kq* factors: accuracy and comparison *Med. Phys.* **38** 4600–9
Muir B, Xiong G, Selvam T P and Rogers D W O 2009 ^{60}Co phase-space files generated using BEAMnrc *Technical Report* CLRP-09-01 Physics Department, Carleton University
Picard S, Burns D T, Roger P, Allisy-Roberts P J, Kapsch R P and Krauss A 2011 Key comparison BIPM. RI(I)-K6 of the standards for absorbed dose to water of the PTB, germany and the BIPM in accelerator photon beams *Metrologia* **48** 06020
Picard S, Burns D T, Roger P, Allisy-Roberts P J, McEwen M R, Cojocaru C D and Ross C K 2010 Comparison of the standards for absorbed dose to water of the NRC and the BIPM for accelerator photon beams *Metrologia* **47** 06025
Picard S, Burns D T, Roger P, Delaunay F, Gouriou J, Roy M L, Ostrowsky A, Sommier L and Vermesse D 2013 Key comparison BIPM. RI(I)-K6 of the standards for absorbed dose to water of the LNE–LNHB, france and the BIPM in accelerator photon beams *Metrologia* **50** 06015
Pimpinella M, Silvi L and Pinto M 2019 Calculation of kq factors for farmer-type ionization chambers following the recent recommendations on new key dosimetry data *Phys. Med.* **57** 221–30
Salvat F 2015 PENELOPE-2014: a code system for Monte Carlo simulation of electron and photon transport *Technical Report* NEA/NSC/DOC(2015)3 Nuclear Energy Agency
Sempau J and Andreo P 2006 Configuration of the electron transport algorithm of PENELOPE to simulate ion chambers *Phys. Med. Biol.* **51** 3533–48
Sempau J, Andreo P, Aldana J, Mazurier J and Salvat F 2004 Electron beam quality correction factors for plane-parallel ionization chambers: Monte Carlo calculations using the PENELOPE system *Phys. Med. Biol.* **49** 4427–44
Sempau J, Badal A and Brualla L 2011 A PENELOPE-based system for the automated Monte Carlo simulation of clinacs and voxelized geometries—application to far-from-axis fields *Med. Phys.* **38** 5887–95
Sempau J, Sánchez-Reyes A, Salvat F, ben Tahar H O, Jiang S B and Fernández-Varea J M 2001 Monte Carlo simulation of electron beams from an accelerator head using PENELOPE *Phys. Med. Biol.* **46** 1163–86
Swanpalmer J and Johansson K A 2011 Experimental investigation of the effect of air cavity size in cylindrical ionization chambers on the measurements in ^{60}Co radiotherapy beams *Phys. Med. Biol.* **56** 7093–107
Swanpalmer J and Johansson K A 2012 The effect of air cavity size in cylindrical ionization chambers on the measurements in high-energy radiotherapy photon beams—an experimental study *Phys. Med. Biol.* **57** 4671–81
Wang L L W and Rogers D W O 2008 Calculation of the replacement correction factors for ion chambers in megavoltage beams by Monte Carlo simulation *Med. Phys.* **35** 1747–55
Wang L L W and Rogers D W O 2009 The replacement correction factors for cylindrical chambers in high-energy photon beams *Phys. Med. Biol.* **54** 1609–20
Wulff J, Heverhagen J T and Zink K 2008a Monte-Carlo-based perturbation and beam quality correction factors for thimble ionization chambers in high-energy photon beams *Phys. Med. Biol.* **53** 2823–36
Wulff J, Heverhagen J T, Zink K and Kawrakow I 2010 Investigation of systematic uncertainties in Monte Carlo-calculated beam quality correction factors *Phys. Med. Biol.* **55** 4481–93
Wulff J, Zink K and Kawrakow I 2008b Efficiency improvements for ion chamber calculations in high energy photon beams *Med. Phys.* **35** 1328–36